0511E

EUROPEAN ORGANIZATION FOR NUCLEAR RESEARCH
CERN - SPS DIVISION

CERN/SPS/85-2 (DI-MST)

TRANSVERSE MODE COUPLING INSTABLITIES IN THE SPS

Yong-Ho Chin

Prévessin - 12th February, 1985

CONTENTS

I. Introduction

It has been established by many studies that transverse fast instabilities, which have been observed in large electron storage rings such as PETRA[1] and PEP[2], are explained by coupling of coherent modes in phase space. Both analytical methods[3,4] starting with the Vlasov equation and computer simulations[4,5] give good agreement with experimental results if the appropriate transverse impedance is known. On the contrary, such a fast transverse instability has so far not been normally observed in proton rings. For example, the tune shift $\Delta\nu_o$ of the lowest head-tail mode m = o at SPS is about 5 times bigger than the synchrotron tune ν_s, but no fast instability has been observed to occur[6]. Even if it is unreasonable to simply apply the empirical rule of thumb $\Delta\nu_o \sim \nu_s$ to determine the threshold, it seems to be hard to think that no two modes cross anywhere. A major difference between a proton and an electron beam is in the bunch length; that is, a proton bunch is usually much longer than an electron bunch. Therefore, the bunch length may be the reason why the mode-coupling instability does not occur in proton beams.

However, there is another puzzle. In the process to solve the Vlasov equation, we introduce "higher radial modes" in addition to usual "azimuthal modes" (which depends on the model of the particle distribution function assumed. For example, only azimuthal modes appear in a hollow-beam model[7]). The infinite number of higher radial modes is degenerate for the tune $\nu_\beta + m\nu_s$ (ν_β = betatron tune, m = integer) at zero beam intensity. As the intensity increases, the degeneracy is removed, and the modes cluster near $m\nu_s$. The frequencies are so close to each other that it seems to be easy for them to couple. If so, that coupling would give a much lower threshold than two modes with different azimuthal mode numbers. However, experimental observation and computer simulation show that it is not true.

One may draw a conclusion from this, that higher radial modes are harmless in the sense that they cannot couple at all. On the other hand, the author's analysis of mode-coupling instabilities at TRISTAN ring showed that the second lowest radial mode for m = o can couple the m = 1 mode with the lowest radial mode (figure 2 in Ref. 3). The consideration above implies that there exists a "selection rule" for a possible pair of couplings.

The main purpose of the present paper is to show why a mode-coupling instability has not been observed at SPS. We will start with formulating a mode-coupling theory for a Gaussian bunch as a "pure matrix eigenvalue problem" in Sec. II. The method of derivation is well established; however, the formalism used by the author together with Satoh or by Besnier-Brand-Zotter results in a formulation which requires finding the zeroes of an infinite determinant. This is, not only difficult for numerical calculation, but also makes insight into the mechanism of coupling of two modes difficult. The present formalism has the advantage that it is easy to see, from the structure of the eigen matrix, how an arbitrary pair of modes affect each other. We shall derive a selection rule from this matrix argument in Sec. III. Comparison of numerical calculations with the experimental results at SPS for 26 GeV and 315 GeV will be done in Sec. IV. Furthermore, the stability limit for beam intensity at SPS as LEP injection[8] is discussed in Sec. V. Our conclusions are given in Sec. VI.

II. Mode-coupling theory

In this section, we derive a formalism for mode-coupling theory as a "pure eigenvalue problem". Although transverse instabilities are concerned, it is necessary to take into consideration both the transverse and the longitudinal phase spaces. The particle distribution function $\psi(u, du/d\tau, \theta, d\theta/d\tau)$ satisfies the Vlasov equation

$$\frac{\partial \Psi}{\partial \tau} + \dot{u}\ \frac{\partial \Psi}{\partial u} + \ddot{u}\ \frac{\partial \Psi}{\partial \dot{u}} + \dot{\theta}\ \frac{\partial \Psi}{\partial \theta} + \ddot{\theta}\ \frac{\partial \Psi}{\partial \dot{\theta}} = 0, \tag{2.1}$$

where u is the transverse displacement from the beam axis normalized by the square root of the beta-function β_z (z = x,y) :

$$u = \frac{z}{\sqrt{\beta_z(s)}} \tag{2.2}$$

and θ is the longitudinal angular position with respect to the bunch center. The independent variable is the quasi time τ defined by

$$\tau = \frac{1}{\omega_\beta} \int \frac{ds}{\beta_z(s)} \tag{2.3}$$

where ω_β is the angular betatron frequency.

A dot means taking derivative with respect to τ. The evolution of Ψ is governed by equations of motion of a single particle

$$\frac{d^2u}{d\tau^2} + (\omega_\beta - \frac{\xi}{\alpha}\ \omega_o\theta')^2 u = \frac{F_z}{E}\ \omega_\beta^2\ \beta_z^{3/2}, \tag{2.4}$$

$$\frac{d^2\theta}{d\tau^2} + \omega_s^2\theta = 0, \tag{2.5}$$

where F_z is the transverse wake force generated by the dipole moment of a beam. We disregard the longitudinal wake force acting on the longitudinal motion of a particle, which is usually treated separately in the study of longitudinal instabilities. A longitudinal force is also generated by the transverse dipole moment, but it is so small that we neglect it as well[17]. The prime on θ denotes differentiation with respect to θ_L, the angular position around a ring, i.e. θ_L = s/R,

where R is the average radius of a ring. The term $\omega_\xi = \xi\ \omega_o \theta'/\alpha$ represents the fact that the betatron frequency depends on the momentum through the chromaticity ξ. The other symbols are: $\omega_o = (\frac{2\pi}{T})$ is the angular revolution frequency, α is the momentum compaction factor, E is the beam energy, ω_s is the synchrotron oscillation angular frequency.

We then transform the longitudinal and the transverse coordinates into polar coordinates defined by

$$u = r_z \cos \phi_z,$$

$$\frac{du}{d\tau} = -(\omega_\beta - \omega_\xi) r_z \sin d_z,$$

$$\theta = r \cos \phi ,$$

$$\frac{d\theta}{d\tau} = -\omega_s\ r \sin \phi \quad . \tag{2.6}$$

With these transformations, the Vlasov equation (2.1) becomes

$$\frac{\partial \psi}{\partial \tau} + (\omega_\beta - \frac{\xi}{\alpha}\omega_o\theta')\frac{\partial \psi}{\partial \phi_z} + \omega_s \frac{\partial \psi}{\partial \phi} + \frac{F_z}{E}\omega_\beta^2 \beta_z^{3/2}\frac{\partial \psi}{\partial \dot{u}} = 0 . \tag{2.7}$$

Here we change the independent variable from τ to θ_L, for it is at a fixed location in a ring that the dipole current is observed and hence it is more convenient to think in the frequency domain with respect to θ_L, instead of τ which had a merit to make the description of equations of motion simpler.

Using the relation

$$\frac{\partial}{\partial \tau} = \omega_\beta \frac{\beta_z}{R}\frac{\partial}{\partial \theta_L} , \tag{2.8}$$

we get

$$\omega_o \frac{\partial \psi}{\partial \theta_L} + (\omega_\beta - \frac{\xi}{\alpha} \omega_o \theta') \frac{\partial \psi}{\partial \phi_z} + \omega_s \frac{\partial \psi}{\partial \phi} + \frac{F_z}{E} \beta_z^{1/2} R \omega_o \omega_\beta \frac{\partial \psi}{\partial u} = 0 . \quad (2.9)$$

In this expression, we have averaged β_z^{-1} over the ring except in the last term which stands for the source term of the transverse force. In general wake forces F_z are generated at localized places, and one should take β_z at those points in order to express properly how much they act back to the beam.

If the perturbation to the beam is small, we can decompose the distribution function ψ into an unperturbed part, which is a function of r and r_z only, and a perturbed part

$$\psi = f_o(r_z)\, g_o(r) + f(r_z, \phi_z)\, g(r,\phi)\, e^{-i \frac{\Omega}{\omega_o} \theta_L + i \frac{\xi}{\alpha} \theta} , \quad (2.10)$$

where Ω is the mode frequency to be determined, and $\exp(i\xi\theta/\alpha)$ is the head-tail phase factor. Substituting Eq. (2.10) into the Vlasov eq. (2.9), and linearizing it with respect to the perturbation terms, we obtain

$$\left[-i\Omega f g + \omega_\beta \frac{\partial f}{\partial \phi_z} g + \omega_s f \frac{\partial g}{\partial \phi}\right] e^{-i \frac{\Omega}{\omega_o} \theta_L + i \frac{\xi}{\alpha} \theta} - \frac{F_z}{E} \beta_z^{1/2} R \omega_o \sin \phi_z \frac{df_o}{dr_z} \cdot g_o = 0. \quad (2.11)$$

Let us now consider the transverse force F_z. The dipole current observed at location θ_L as as functic: of θ is written as

$$\omega_o D\, \rho\,(\theta)\, e^{-i\frac{\Omega}{\omega_o}\theta_L + i\frac{\xi}{\alpha}\theta}\,, \tag{2.12}$$

where $\rho(\theta)$ is the longitudinal charge distribution:

$$\rho(\theta) = \int_{-\infty}^{\infty} g\,(r,\phi)\,d\theta \tag{2.13}$$

and D is the transverse dipole moment:

$$D = \sqrt{\beta_z}\;\frac{\iint u\, f\,(r_z,\phi_z)\, r_z d\, r_z\, d\phi_z}{\iint f_o(r_z)\, r_z\, dr_z\, d\phi_z} = \sqrt{\beta_z}\cdot D_n\,. \tag{2.14}$$

We want to express the dipole current as a signal in time which the impedance or the wake function picks up. Including multipole passage effects and going to the frequency domain with Fourier transform of $\rho(\theta)$

$$\tilde{\rho}\,(p) = \frac{1}{2\pi}\int e^{-ip\theta}\rho(\theta)\,d\theta$$

$$= \frac{\omega_s}{2\pi}\iint e^{-ipr\cos\phi}\, g(r,\phi)\, rd\, rd\phi\,, \tag{2.15}$$

we have the dipole current as

$$\omega_o \sqrt{\beta_z} D_n \sum_{p=-\infty}^{\infty} \tilde{\rho}\,(p + \frac{\Omega}{\omega_o} - \frac{\xi}{\alpha})\, e^{-i(p+\frac{\Omega}{\omega_o})\omega_o t}\,. \tag{2.16}$$

The transverse force F_z felt at a location θ is thus expressed by

$$F_z = \frac{ie}{2\pi R}\,\omega_o \sqrt{\beta_z}\, D_n e^{-i\frac{\Omega}{\omega_o}\theta_L} \sum_p \tilde{\rho}\,(p + \frac{\Omega}{\omega_o} - \frac{\xi}{\alpha})\, Z_T\,(p + \frac{\Omega}{\omega_o})\, e^{i(p+\frac{\Omega}{\omega_o})\,\theta} \tag{2.17}$$

with the transverse impedance $Z_T(p + \frac{\Omega}{\omega_o})$ at frequency $\omega = p\omega_o + \Omega$.

The symbol e means the elementary charge. Inserting Eq. (2.17) into Eq. (2.11), we obtain

$$[-i\Omega fg + \omega_\beta \frac{\partial f}{\partial \phi_z} g + \omega_s f \frac{\partial g}{\partial \phi}] \, e^{i(\frac{\xi}{\alpha} - \frac{\Omega}{\omega_o})\theta}$$

$$- i\frac{D_n \beta_z}{T \, E/e} \, \omega_o \sum_p Z_T(p + \frac{\Omega}{\omega_o}) \, \tilde{\rho} \, (p + \frac{\Omega}{\omega_o} - \frac{\xi}{\alpha}) \, e^{ip\theta} \, g_o \sin \phi_z \frac{df_o}{dr_z} = 0 \, . \tag{2.18}$$

Here we expand $\sin \phi_z$ with $\exp(i\phi_z)$ and $\exp(-i\phi_z)$.

If the mode frequency shifts are small compared to ω_β, we can ignore the $\exp(i\phi_z)$ term. The solution for f is easily found:

$$f = - D_n \frac{df_o}{dr_z} \exp(i\phi_z) \, . \tag{2.19}$$

The Vlasov equation then reduces to

$$[-i(\Omega - \omega_\beta) + \omega_s \frac{\partial}{\partial \phi}] \, g + \frac{\beta_z \omega_o}{2TE/e} \sum_p Z_T(p + \frac{\Omega}{\omega_o}) \, \tilde{p} \, (p + \frac{\Omega}{\omega_o} - \frac{\xi}{\alpha}) e^{i(p + \frac{\Omega}{\omega_o} - \frac{\xi}{\alpha_o})\theta} \, g_o = 0 \, . \tag{2.20}$$

Since $g(r,\phi)$ has to be periodic in ϕ with period 2π, we can expand it as

$$g(r,\phi) = \sum_{m=-\infty}^{\infty} g_m(r) \exp(im\phi), \tag{2.21}$$

where m is the azimuthal mode number.

Substituting Eq. (2.21) into Eq. (2.20), and integrating over ϕ after multiplying by $\exp(-im\phi)$ on both sides, we get

$$(\lambda - m)g_m(r) = -i \frac{\beta_z \omega_o}{2\ TE/e\omega_s^2 g_o} \sum_p Z_T(p + \frac{\Omega}{\omega_o}) \tilde{\rho} (p + \frac{\Omega}{\omega_o} - \frac{\xi}{\alpha}) \times i^m J_m((p + \frac{\Omega}{\omega_o} - \frac{\xi}{\alpha}) r), \quad (2.22)$$

where

$$\lambda = \frac{\Omega - \omega_\beta}{\omega_s} . \quad (2.23)$$

In obtaining Eq. (2.22), we have used the formula[9)]

$$\int_o^{2\pi} e^{ipr \cos \phi - m\phi} d\phi = 2\pi i^m J_m(pr) \quad (2.24)$$

Using the same formula, one gets

$$\tilde{\rho}(p + \frac{\Omega}{\omega_o} - \frac{\xi}{\alpha}) = \omega_s \sum_{n=-\infty}^{\infty} i^{-n} \int_o^\infty g_n(r) J_n ((p + \frac{\Omega}{\omega_o} - \frac{\xi}{\alpha})r) rdr. \quad (2.25)$$

Inserting Eq. (2.25) into Eq. (2.22), we obtain an equation for g_m

$$(\lambda-m)g_m(r) = -i \frac{\beta_z \omega_o}{2TE/e} g_o \sum_p Z_T(p + \frac{\Omega}{\omega_o}) i^m J_m((p + \frac{\Omega}{\omega_o} - \frac{\xi}{\alpha}) r) \times \sum_{n=-\infty}^{\infty} i^{-n} \int_o^\infty g_n (r') J_n((p + \frac{\Omega}{\omega_o} - \frac{\xi}{\alpha})r')r'dr' \quad (2.26)$$

which is Sacherer's integral equation including mode coupling. (Note the summation about n).

We solve Eq. (2.26) by expanding $g_m(r)$ in orthogonal functions. Looking at Eq. (2.26) carefully, we notice that the functional dependence of $g_m(r)$ is the same for positive and negative m, i.e.

$$(\lambda - m)g_m(r) = (\lambda + m)g_{-m}(r) \ . \tag{2.27}$$

This implies that we can expand $g_m(r)$ with the same orthogonal functions for positive and negative m as [10]

$$g_m(r) = w(r) \sum_{k=0}^{\infty} a_k^{(m)} f_k^{(|m|)}(r) \ . \tag{2.28}$$

The weight function w(r) is proportional to the unperturbed distribution function

$$w(r) = C\, g_o(r) \tag{2.29}$$

and the functions $f_k^{(|m|)}(r)$ satisfy the following orthogonal relations

$$\int_o^{\infty} w(r)\, f_k^{(|m|)}(r)\, f_\ell^{(|m|)}(r)\, r dr = \delta_{k\ell} . \tag{2.30}$$

Insertion of Eq. (2.28) into Eq. (2.26) leads to

$$(\lambda - m)w(r) \sum_{k=0}^{\infty} a_k^{(m)}\, f_k^{(|m|)}(r) = - i\, \frac{\beta_z \omega_o}{2TE/e} \cdot \frac{w(r)}{C}$$

$$\times \sum_p Z_T \left(p + \frac{\Omega}{\omega_o}\right) i^m J_m\left(\left(p + \frac{\Omega}{\omega_o} - \frac{\xi}{\alpha}\right)r\right)$$

$$\times \sum_{n=-\infty}^{\infty} i^{-n} \int_o^{\infty} w(r') \sum_{\ell=0}^{\infty} a_\ell^{(n)} f_\ell^{(|n|)}(r')\, J_n\left(\left(p + \frac{\Omega}{\omega_o} - \frac{\xi}{\alpha}\right)r'\right) r'\, dr' \tag{2.31}$$

Multiply $f_k^{(|m|)}(r)$ and integrate Eq. (2.31), and we finally get the matrix eigenvalue equation

$$(\lambda - m)a_k^{(m)} = \sum_{n=-\infty}^{\infty} \sum_{\ell=0}^{\infty} M_{n\ell}^{mk} a_\ell^{(n)}, \tag{2.32}$$

where

$$M_{n\ell}^{mk} = -iK \sum_p Z_T(p + \frac{\Omega}{\omega_o}) i^{m-n} I_{mk}(p + \frac{\Omega}{\omega_o} - \frac{\xi}{\alpha}) I_{n\ell}(p + \frac{\Omega}{\omega_o} - \frac{\xi}{\alpha}), \tag{2.33}$$

$$I_{mk}(p + \frac{\Omega}{\omega_o} - \frac{\xi}{\alpha}) = \int_o^\infty w(r) f_k^{(|m|)}(r) J_m((p + \frac{\Omega}{\omega_o} - \frac{\xi}{\alpha})r)rdr, \tag{2.34}$$

and

$$K = \frac{\beta_z \omega_o}{2TE/e\ C}. \tag{2.35}$$

The non-trivial solutions of Eq. (2.32) for $a_k^{(m)}$ require that

$$\det(\lambda I - A) = 0, \tag{2.36}$$

where I is a unit matrix, and A is the matrix with elements

$$A_{n\ell}^{mk} = m\delta_{mn}\delta_{k\ell} + M_{n\ell}^{mk}. \tag{2.37}$$

Equation (2.36) is a "pure matrix eigenvalue equation" of λ. This form is very convenient for numerical calculations. The "interaction matrix" M has the following characteristics:

$$M_{n\ell}^{-mk} = M_{-n\ell}^{mk} = M_{n\ell}^{mk} \tag{2.38}$$

and

$$M_{n\ell}^{mk} = (-1)^{m-n} M_{mk}^{n\ell}. \tag{2.39}$$

It remains to find appropriate orthogonal functions. The normalization factor C and the orthogonal functions depend on the unperturbed distribution function assumed, so to proceed further, we assume a Gaussian distribution

$$g_o(r) = \frac{Ne}{2\pi\omega_s\sigma^2} e^{-\frac{r^2}{2\sigma^2}} , \qquad (2.40)$$

where N is the number of particles per bunch and σ is the bunch length in θ unit ($= \sigma_z/R$). After some easy considerations, we notice that the normalization factor C can be arbitrarily chosen, namely, a different choice of C leads only to change of the definition of $f_k^{(|m|)}(r)$. To get a simple expression, we chose

$$C = \frac{2\pi\omega_s}{Ne} \qquad (2.41)$$

and then [9]

$$f_k^{(|m|)}(r) = \left(\frac{k!}{(|m| + k)!}\right)^{\frac{1}{2}} \left(\frac{r}{\sqrt{2}\sigma}\right)^{|m|} L_k^{(|m|)}\left(\frac{r^2}{2\sigma^2}\right) , \qquad (2.42)$$

and where $L_k^{(|m|)}$ is the generalized Laguerre polynomials.[9].

The function $I_{mk}(p')$ becomes

$$I_{mk}(p') = \frac{\varepsilon_m}{\sqrt{(|m| + k)!k!}} \left(\frac{p'\sigma}{\sqrt{2}}\right)^{|m|+2k} \exp\left(-\frac{(p'\sigma)^2}{2}\right) , \qquad (2.43)$$

where

$$\varepsilon_m = 1 \qquad \text{for } m \geq 0$$
$$= (-1)^m \qquad \text{for } m < 0 \quad .$$

The apparent form of the scaling factor K is

$$K = \frac{Ne\beta_z\omega_0}{4\pi T\omega_s E/e} \quad . \tag{2.44}$$

III. Selection Rule

Information about a selection rule is contained in the structure of the matrix M. Two arbitrary modes, each of which is specified only by the azimuthal mode number m and the radial mode number k at zero beam intensity, come to have the other party's component through the "interaction matrix M" at a finite intensity. Let us limit the discussion to the 2 x 2 matrix containing the modes concerned. Besides, we continue our discussion with a Gaussian distribution, without losing any essentials. Supposing a broad-band impedance, the matrix element can be approximated as

$$M^{mk}_{n\ell} = -iK \sum_{p=-\infty}^{\infty} Z_T(p)\, i^{m-n}\, I_{mk}(p\sigma)\, I_{n\ell}(p\sigma)$$

$$= -iK \sum_{p} Z_T(p)\, i^{m-n} \frac{\epsilon_m}{\sqrt{(|m|+k)!\,k!}} \frac{\epsilon_n}{\sqrt{(|n|+\ell)!\,\ell!}} \left(\frac{p\sigma}{\sqrt{2}}\right)^{|m|+|n|+2(k+\ell)} \exp(-p^2\sigma^2) \quad . \tag{3.1}$$

The real and imaginary parts of the impedance are an odd and an even function of the frequency $p\omega_o$, respectively. Therefore, in the case that m and n have the same polarity (i.e. m-n = even), only the imaginary part of the impedance is left after summation over p. In the opposite case, (m-n = odd), only the real part remains. All the matrix elements are real quantities. It should be noted that the radial mode number k and ℓ play no role in this polarity discussion; they always contribute to summation as even functions, since they are multiplied by a factor 2.

First, we consider the case of m-n = odd. Two mode frequencies are given by the determinant of the 2 X 2 matrix:

$$\begin{vmatrix} \lambda - m - M_{mk}^{mk} & - M_{n\ell}^{mk} \\ - M_{mk}^{n\ell} & \lambda - n - M_{n\ell}^{n\ell} \end{vmatrix} = 0 \quad . \tag{3.2}$$

The solutions are

$$\lambda_{1,2} = \frac{1}{2}\left(m + M_{mk}^{mk} + n + M_{n\ell}^{n\ell}\right) \pm \frac{1}{2}\sqrt{\left(m + M_{mk}^{mk} - n - M_{n\ell}^{n\ell}\right)^2 - 4\, M_{n\ell}^{mk^2}} \quad , \tag{3.3}$$

where $M_{mk}^{n\ell}$ has been replaced by $- M_{n\ell}^{mk}$. When two values, $m + M_{mk}^{mk}$ and $n + M_{n\ell}^{n\ell}$, get very close, the term under the square root can become negative, and the two solutions become complex conjugate. The physical meaning of what happens is that the two modes cross, and they become unstable (one of which becomes stable), that is, a mode-coupling instability happens. The case of m-n = even can be treated in the same way; the difference is that $M_{mk}^{n\ell}$ should be replaced by $M_{n\ell}^{mk}$. The conclusion, however, becomes just opposite. The solutions are

$$\lambda_{1,2} = \frac{1}{2}\left(m + M_{mk}^{mk} + n + M_{n\ell}^{n\ell}\right) \pm \frac{1}{2}\sqrt{\left(m + M_{mk}^{mk} - n - M_{n\ell}^{n\ell}\right)^2 + 4\, M_{n\ell}^{mk2}} \quad . \tag{3.4}$$

The inside of the square root is always positive; the two modes have different frequencies and never cross.

When the solutions are shown graphically, the difference of behaviour of mode frequencies in the two cases is seen more clearly.

Figure 1(a) and (b) show these results as a function of the scaling factor K. In this example, numerical values of the matrix elements are taken as follows: $M^{mk}_{mk} = -2K$, $M^{mk}_{n\ell} = .5K$, $M^{n\ell}_{n\ell} = 0$. As is evident from the figures, the case of m-n = odd, Fig. 1 (a) shows that the two modes attract each other to merge, while in the case of m-n = even, they repel each other; the upper mode going down is bent to the right when it approaches the lower mode.

We should pay special attention to the interpretation of the latter case. The mode starting from $\lambda = m$ is repelled also from the infinite number of other higher radial modes at the $\lambda = n$ line. One may ask then if that mode cannot exceed the line $\lambda = n$. The answer is yes. In order to see it, we must investigate the behaviour of the eigenvectors corresponding to the eigen values (3.4). They are:

$$\begin{pmatrix} a^{(m)}_k \\ a^{(n)}_\ell \end{pmatrix}_{1,2} = \frac{1}{\sqrt{M^{mk\,2}_{n\ell} + (\lambda_{1,2}-m-M^{mk}_{mk})^2}} \begin{pmatrix} M^{mk}_{n\ell} \\ \lambda_{1,2}-m-M^{mk}_{mk} \end{pmatrix} . \qquad (3.5)$$

The amplitudes are normalized to unity. Figure 2 shows plots of numerical values. Each mode which starts with one side's component loses its original component and comes to contain the other side's as the intensity increases. Around the point where the eigenvalues are bent, the ratio of two components is exchanged. It might be meaningless to assign a mode number to each eigen solution, because there exists no "pure" mode any more; however, if we make a rule to define a mode in terms of the azimuthal and the radial mode number corresponding to the expansion function which has the largest expansion coefficient in the eigenvector, we should regard that the mode starting $\lambda = m$ continues to the mode going down below the $\lambda = n$ line. This rule is, of course, useless for many situations vague to judge.

From the experimental point of view, the following statement can be made. Let us explain by a concrete example and schematical figures. The tune shift of the lowest head-tail mode m = 0 is normally much bigger than that of m = -2 mode, (which depends on impedance). Forget the m = -1 mode between them as harmless here. Spectra of a beam when kicked transversely looks like Fig. 3(a) at low intensity. As the intensity increases, the tune of m = 0 mode shifts down, and the m= -2 mode is enhanced due to a mixture of the rigid dipole oscillation, see Fig. 3(b). The intensity increasing further, the signal of the left hand side starts to move largely, while the right signal, which was dipole mode so far, stops moving around the frequency $\omega = \omega_\beta - 2\omega_s$, as shown in Fig. 3(c). The heights of the signals are reversed at the same time, because the left mode contains the component of the rigid dipole oscillation at most; in other words, it is more enhanced by a dipole kick. It is this left signal that is experimentally observed and assigned as continuation of the dipole mode.

In the particular case of m = n, we can draw an interesting conclusion on higher radial modes. Since the radial mode numbers play no role in the matter, we can exactly follow the argument mentioned above for all pairs of k and ℓ. It is therefore concluded that radial modes starting from the same mode frequency cannot couple to each other.

What is stated so far is valid for whatever impedance of a machine. If the real part of the impedance $\mathrm{Re}(Z_T)$ is small at low frequency, as e.g. for a widely used broad-band resonator model, the behaviour of mode coupling is different for long and short bunches. The interaction matrix M consists of the product of the impedance and the bunch spectrum $I_{mk}(p\sigma)\ I_{n\ell}(p\sigma)$. They look like Fig. 4(a) for the m-n = odd case in a short bunch. The overlap between $\mathrm{Re}(Z_T)$ and $I_{mk}(p\sigma)\ I_{n\ell}(p\sigma)$ is not so small that the off-diagonal matrix elements are negligible. The two modes can strongly couple through them.

As the bunch length gets longer, the bunch spectrum shifts to the low frequency part, and the overlap with $Re(Z_T)$ becomes smaller, see Fig. 4(b). In the limit of the zero-overlap, the matrix Eq. (3.2) is diagonalized, and the two modes behave independently as shown in Fig. 5(a). When the off-diagonal terms are small but not zero, the two modes, which are coupled at a certain beam intensity, becomes uncoupled at slightly higher intensity*. (Fig. 5(b)). The growth rate of the instability does not become very large for such a weak coupling. If the spread of the betatron or the synchrotron frequency is big enough, this slow instability will be suppressed by Landau damping. This implies that mode-coupling instabilities are difficult to observe experimentally in long proton bunches, although they may occur in a qualitative sense.

In the case of m-n = even, this phenomenological change does not happen, for the off-diagonal terms contain the imaginary part of the impedance just as the diagonal terms. Even if the bunch lengthens very much, there is still a finite inductive impedance in the low frequency part so that these terms do not vanish.

In the next section, we shall apply these experiences to the SPS as a concrete example.

IV. Verification of experimental observation at SPS

We start with reviewing some experimental facts at SPS. The first estimate of the SPS transverse impedance was obtained by Boussard and Gareyte[12] from the measurements of the head-tail instability growth rates for mode m = 0 at 270 GeV. With a broad-band resonator model and Sacherer's formula (67) in Ref. 13, the result gives Z_T = 18 MΩ/m at the resonance peak (1.3 GHz) and Q = 1. It was, however, pointed out[13] that this impedance yields a discrepancy in the tune shift measured at 26 GeV; the tune shift evaluated with the same formula is - 0.014 at N_p = 10^{11} whereas measurements gave -0.03.

---

* This short period of coupling can ben seen also in Ruggiero's analysis[11] where it is expressed as a gap where no stationary solution is found.

More recently, the impedance was estimated by Linnecar and Scandale[15] from the measurements of the head-tail tune shift for the same m = 0 mode at 315 GeV. The new value was Z_T = 47.7 MΩ/m, f_r = 1.3 GHz, and Q = 1.

The first method is strongly model dependent. In addition, it is difficult to estimate the reduction of the growth rate by Landau damping quantitatively. The second method is more direct, and automatically gives a correct tune shift at 315 GeV. We therefore use the value Z_T = 47.7 MΩ/m from the second experiment, and see whether the mode-coupling theory explains the observational results at 26 GeV.

However, before going to 26 GeV, let us study mode frequencies at 315 GeV. Figure 6(a) and (b) show the results of numerical calculations using Eq. (2.36) and the matrix (2.33). The real part of the eigenvalues, Re(λ), and the growth rates τ^{-1} are plotted versus the number of particles N_p in a bunch. The parameters used in this calculation are listed in the first column of Table I. Seven azimuthal ($|m| \leq 3$) and three radial ($k \leq 2$) modes are included. The number N_p in Linnecar and Scandale's experiment was $7{,}72 \times 10^{10}$. We can read from the figure that the corresponding tune shift for the lowest azimuthal and radial mode is -3.0×10^{-3}, which is in reasonable agreement with the measurement value $- 2.65 \times 10^{-3}$. This should not be taken for granted, because the impedance was determined using the formula [12] derived with a different model and through the rough method to solve the integral eq. (2.26). (The formula itself is not rough!)

In normal operation, N_p is about 1.6×10^{11}/bunch, so it turns out that this working point is just below the threshold given by the first non-negligible coupling between m = 0 and m = - 1 modes. The bunch length at this beam intensity is, however, determined by longitudinal micro-wave instabilities.[16]. If we increase the intensity, the bunch lengthens, thus leading to higher threshold value. As a consequence, it might be difficult to bring the beam intensity onto the threshold.

The results of calculations at 26 GeV are shown in Fig. 7(a) and (b) for Re(λ) and the growth rate τ^{-1}, respectively. In order to see the behaviour of mode frequencies clearly, only the lowest radial mode is included, but the result is almost the same when more radial modes are included. The parameters used are listed in the second column of Table I. As mentioned in Sect. III, we can see the repulsion between modes with the same polarity. Coupling of modes with different polarity is so weak that it is broken before the growth rates increase considerably. The incoherent betatron tune spread due to the space charge effect is as big as 0.05 at 26 GeV[6]. If we assume that Landau damping compensates growth rates up to the value corresponding to this spread, i.e. 1.4 $\times$ 10^3/sec, these weak mode-coupling instabilities will be suppressed and cannot be seen.

What should be noticed here is, that there is an interrupted line running from the top left to the lower right in Fig. 7(a). In fact, inspection of the eigenvector proves that the dipole mode moves actually along this line. The value Re(λ) for the dipole mode at $N_p = 10^{11}$ is - 5.3, which corresponds to a tune shift value of -0.029. This agrees very well with the experimental value of -0.03[17].

These results thus give a very plausible explanation why the mode-coupling instability has not been observed at SPS.

V. Stability limit as LEP injector

Finally, we examine the stability limit at SPS when operated as LEP Injector[8]. A similar analysis was done by Zotter[18] where Z_T = 18 MΩ/m was used as transverse impedance. Proposed beam parameters are summarized in the last column of Table I. At 3.5 GeV, the synchrotron radiation damping time is about 9 sec., so electrons behave more like protons. Figure 8 (a) and (b) show Re(λ) and the growth rate τ^{-1} at σ_z = 16 cm, respectively. Seven azimuthal modes and three radial modes are included in the calculation. The first coupling is seen to

occur between the lowest radial m = 0 and m = -1 modes. If this coupling would define the threshold for stability, the beam intensity would be limited to $N_p = 0.44 \times 10^{10}$, which is half the proposed value $N_p = 0.81 \times 10^{10}$.[8] There is some hope that the instability may be suppressed by the betatron tune spread of ~ 0.01 [19] due to octupole components in the quadrupole magnets*. Nevertheless, damping due to increasing positive chromaticity, which gives a damping time 4.4 msec [19], should counteract this instability. In that case, the next coupling occurs between the m = -2 and m = -3 modes. This results in a much bigger growth rate and therefore defines the threshold. However, its value of $N_p = 0.7 \times 10^{10}$ is still below the designed one. Even if we change the bunch length, fixing the phase space area like in protons, the threshold is not improved sufficiently, (see Fig. 9). One way to avoid this limitation would be to reduce the number of particles in a bunch by doubling the injection cycles.

VI. Conclusions

We have seen that the transverse mode-coupling theory derived in the present study explains the experimental results at SPS very well. The problem is formulated a pure matrix eigenvalue problem which has several advantages such as convenience in numerical calculations. The largest advantage is that considerations about the structure of the matrix provide us with the selection rule for which pair of modes will be coupled. It is also found that, even if two modes cross for a long bunch, their coupling may be so weak that a slight increase in beam intensity will decouple them. The growth rates may thus stay within the range compensated by Landau damping or other damping mechanism.

---

* This is a dangerous game. If we apply the rule-of-thumb criterion for stability[13] |spread in betatron frequencies| > |coherent frequency shift|, since the real part of the tune shift is already as big as -0.018, i.e. the coherent frequency will be shifted out of the incoherent band -0.01, we might not be able to expect Landau damping.

The calculations for the SPS lead to some suggestions:

- When the SPS is operated as LEP injector for proposed beam parameters, the threshold beam intensity is below the planned value. The injection cycles should therefore be doubled for safety.

- For ppbar operation at 415 GeV, the threshold beam intensity is close to the intensity in normal operation. If some objects are installed which enhance only the transverse impedance without contributing substantially the longitudinal impedance so that the bunch does not lengthen, it may be possible to observe the mode-coupling instability at the SPS already with present beam intensities.

Acknowledgements

The author wishes to thank B. Zotter for helpful discussions and careful reading of the manuscript. He also would like to thank J. Gareyte and L. Evans for their interest in this work and useful information about experimental data at the SPS.

References

1. R.D. Kohaupt, Proc. 11th Int. Conf. on High-Energy Accelerators, CERN. (Birkhäuser Verlag, Basel, 1980), p. 562.

2. PEP Group, Proc. 12th Int. Conf. on High-Energy Accelerators, Fermilab (Chicago, 1983), p. 209.

3. Y. Chin and K. Satoh, IEEE Trans. Nucl. Sci. NS-30, No. 4, 2566 (1983).

4. G. Besnier, D. Brandt and B, Zotter, CERN LEP-TH/84-11, 1984.

5. R.H. Siemann, Nucl. Instrum. Methods, 221, 293 (1984).

6. L.R. Evans, CERN SPS/84-8 (DI-MST), 1984.

7. A.W. Chao, AIP Conference Proceedings No. 105, 353 (1982)

8. The LEP Injector Study Group, LEP Design Report, CERN/SPS/83-26, 1983

9. M. Abramowitz and I.A. Stegun, Handbook of Mathematical Functions, (Dover, New York, 1965).

10. T. Suzuki, Y. Chin and K. Satoh, Part. Accelerators, 13, 179 (1983).

11. F. Ruggiero, CERN-LEP-TH/84-21, 1984.

12. D. Boussard and J. Gareyte, SPS Improvement Report No. 181, 1980.

13. F. Sacherer, in proceedings of the First Course of the International School of Particle Accelerators of the 'Ettore Majorana' Center for Scientific Culture, edited by M.H.Blewett (Erice 1976), CERN Report 77-13, p. 198.

14. J. Gareyte, SPS Improvement Report No. 190. 1982.

15. T. Linnecar and W. Scandale, SPS/DI-MST/ME/84-12, 1984.

16. L. R. Evans, private communication.

17. J. Gareyte, SPS/DI/MST/Note 82-1, 1982

18. B. Zotter, LEP Note 418, 1982.

19. J. Gareyte, private communication.

Table I

Parameters for SPS at various energy

E : beam energy (GeV)	315	26	3.5
ν_s : synchrotron tune	.005	.0055	.013
$\bar{\beta}$: average beta-function (m)	40	40	41.4
σ_z : bunch length (cm)	18	30	16

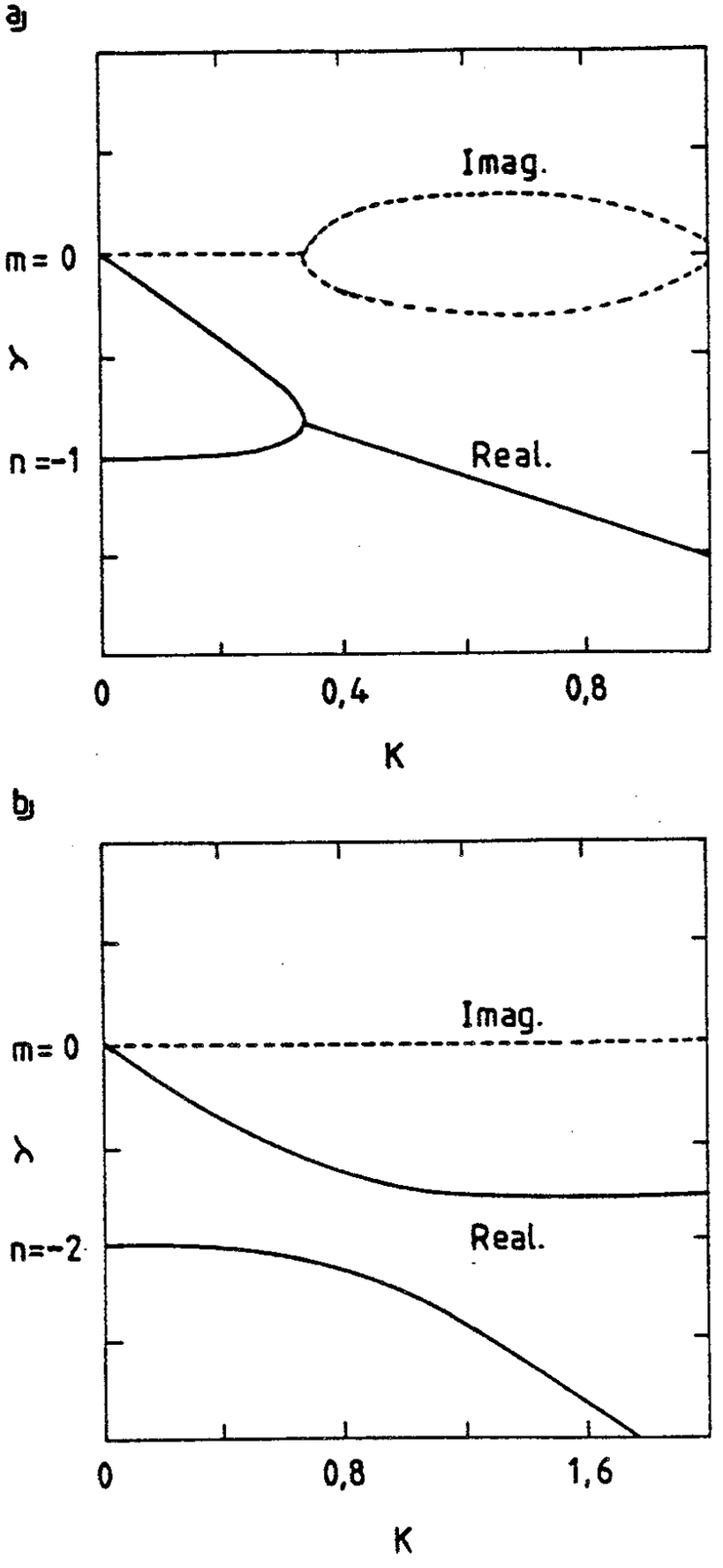

Fig. 1. Eigenvalues as a function of K for the case (a) m - n = odd and (b) m - n = even.

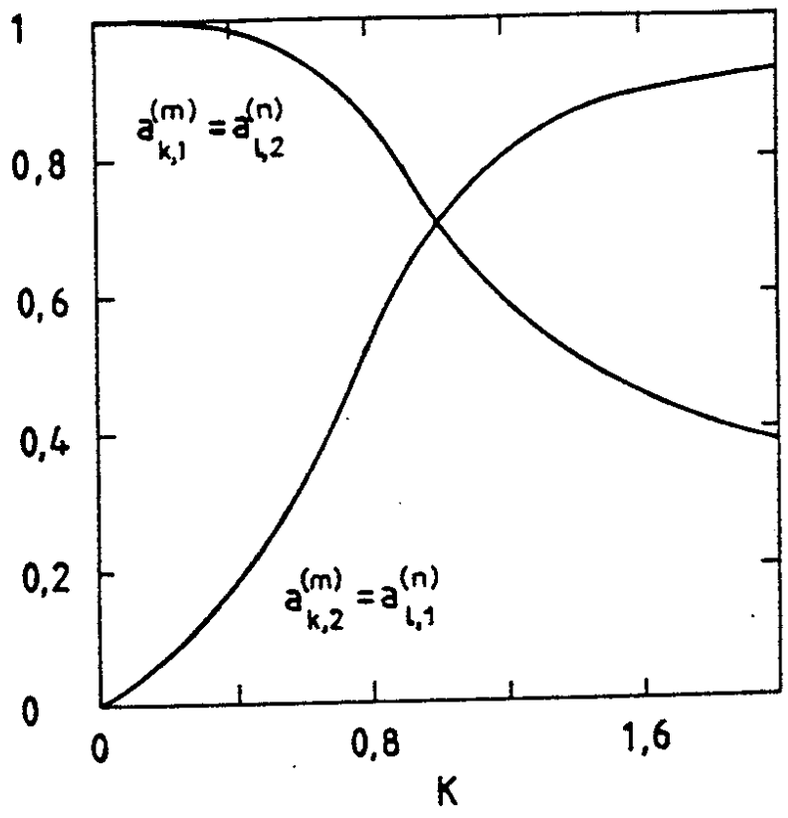

Fig. 2. Eigenvectors for the case (b) m - n = even in Fig. 1.

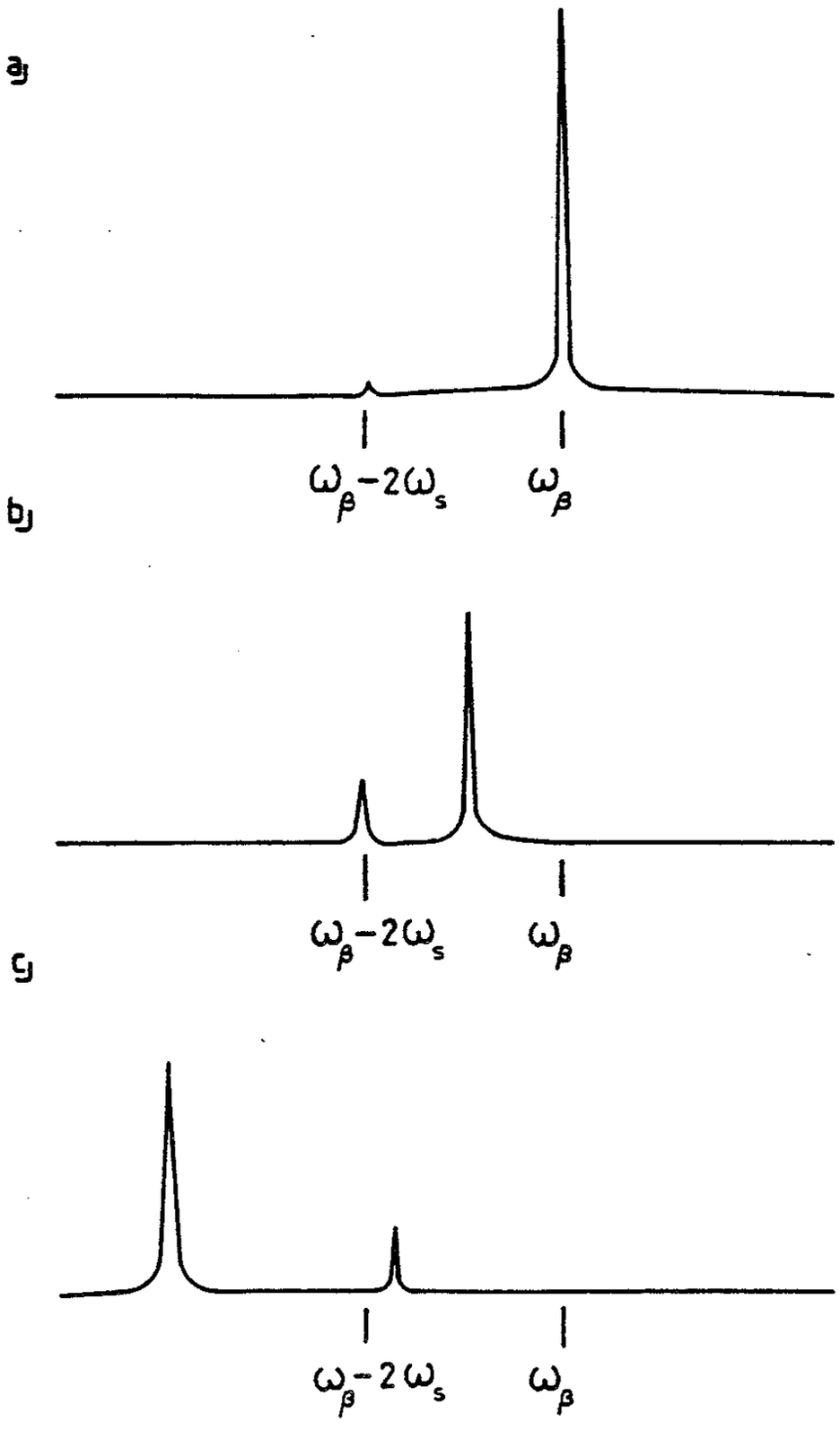

Fig. 3. Sketches of spectra of dipole oscillation for various beam intensities.

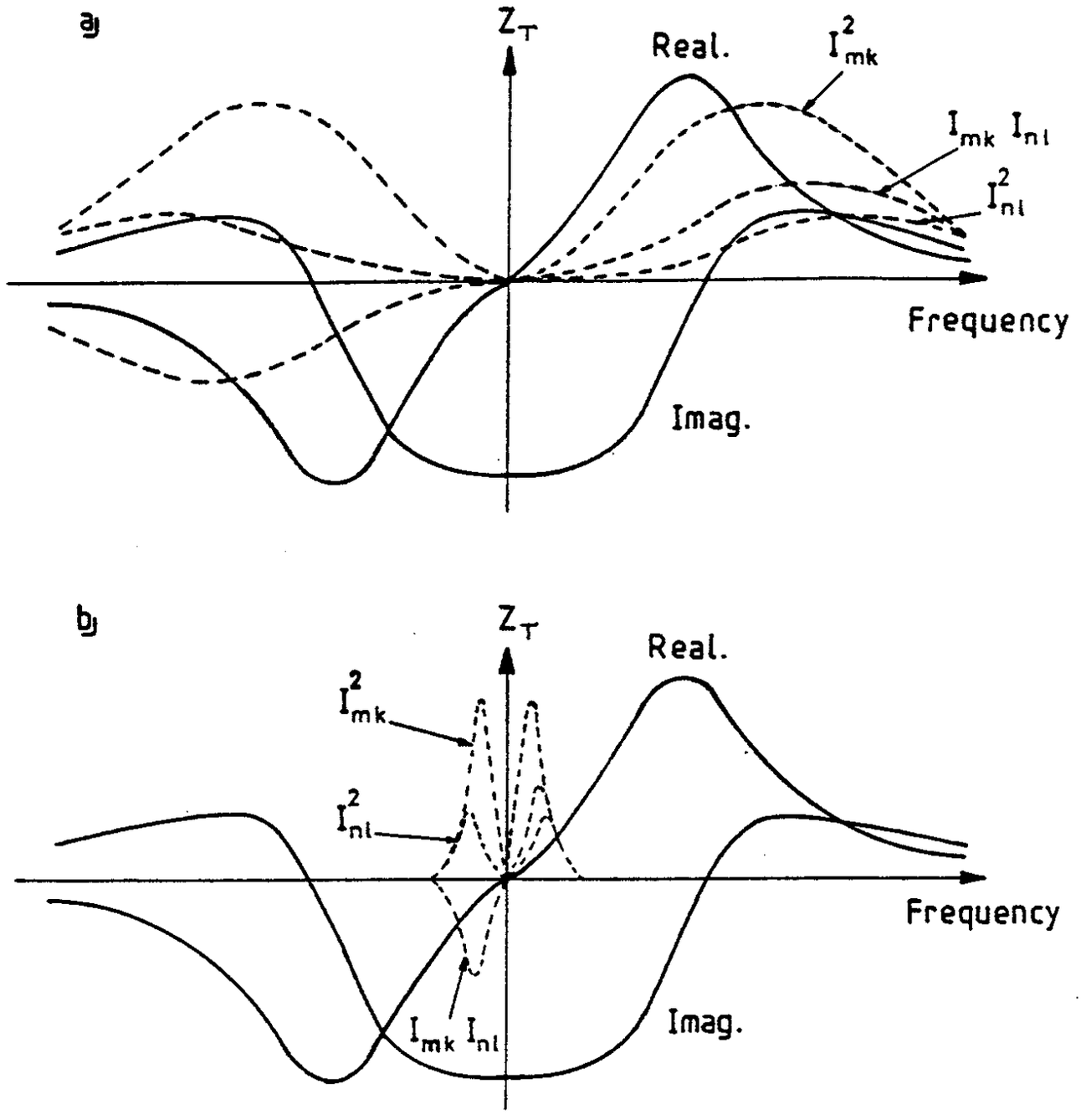

Fig. 4. Broad-band impedance and some bunch spectra versus frequency for (a) a short bunch, (b) a long bunch.

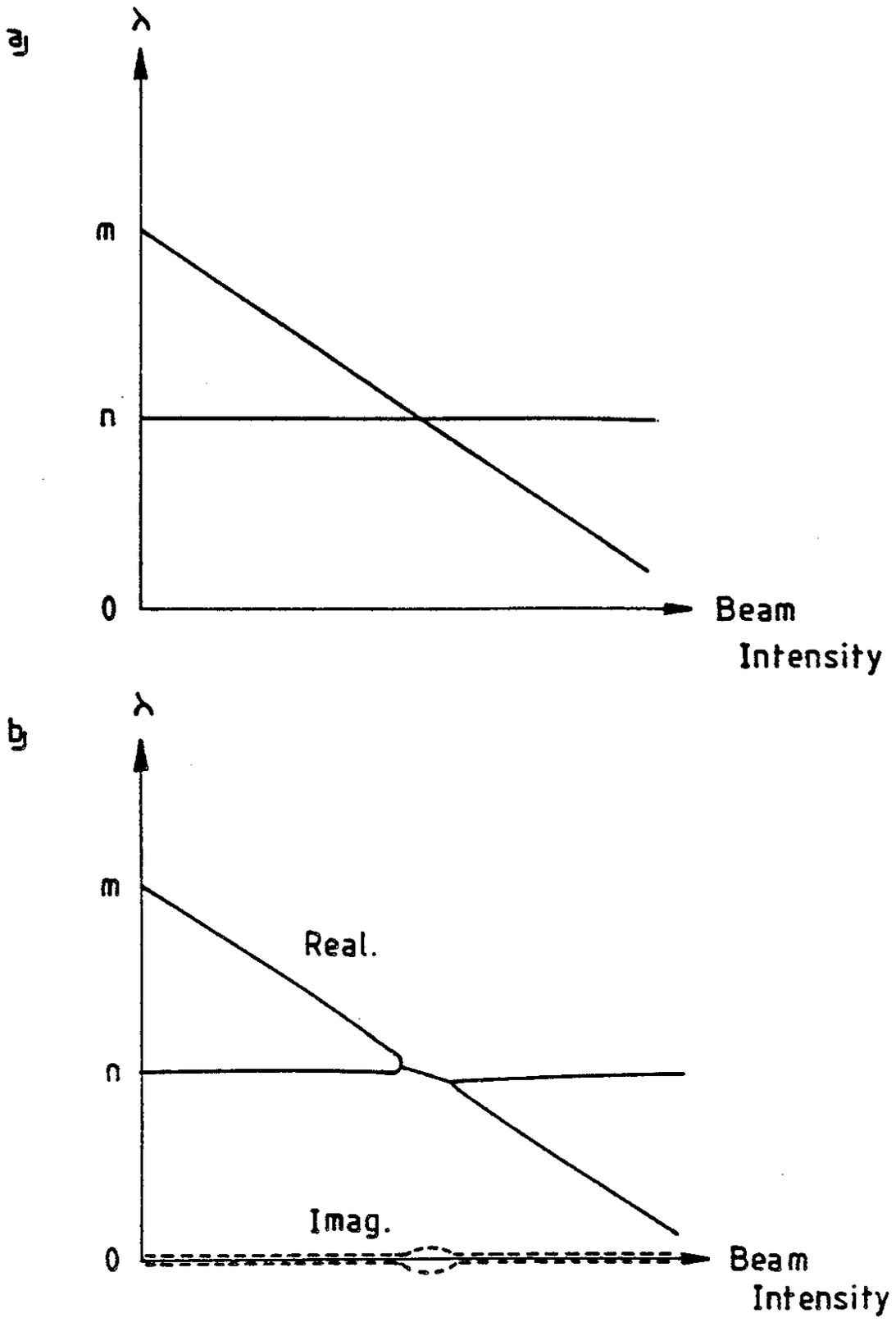

Fig. 5. Mode frequencies when off-diagonal elements are (a) zero and (b) small.

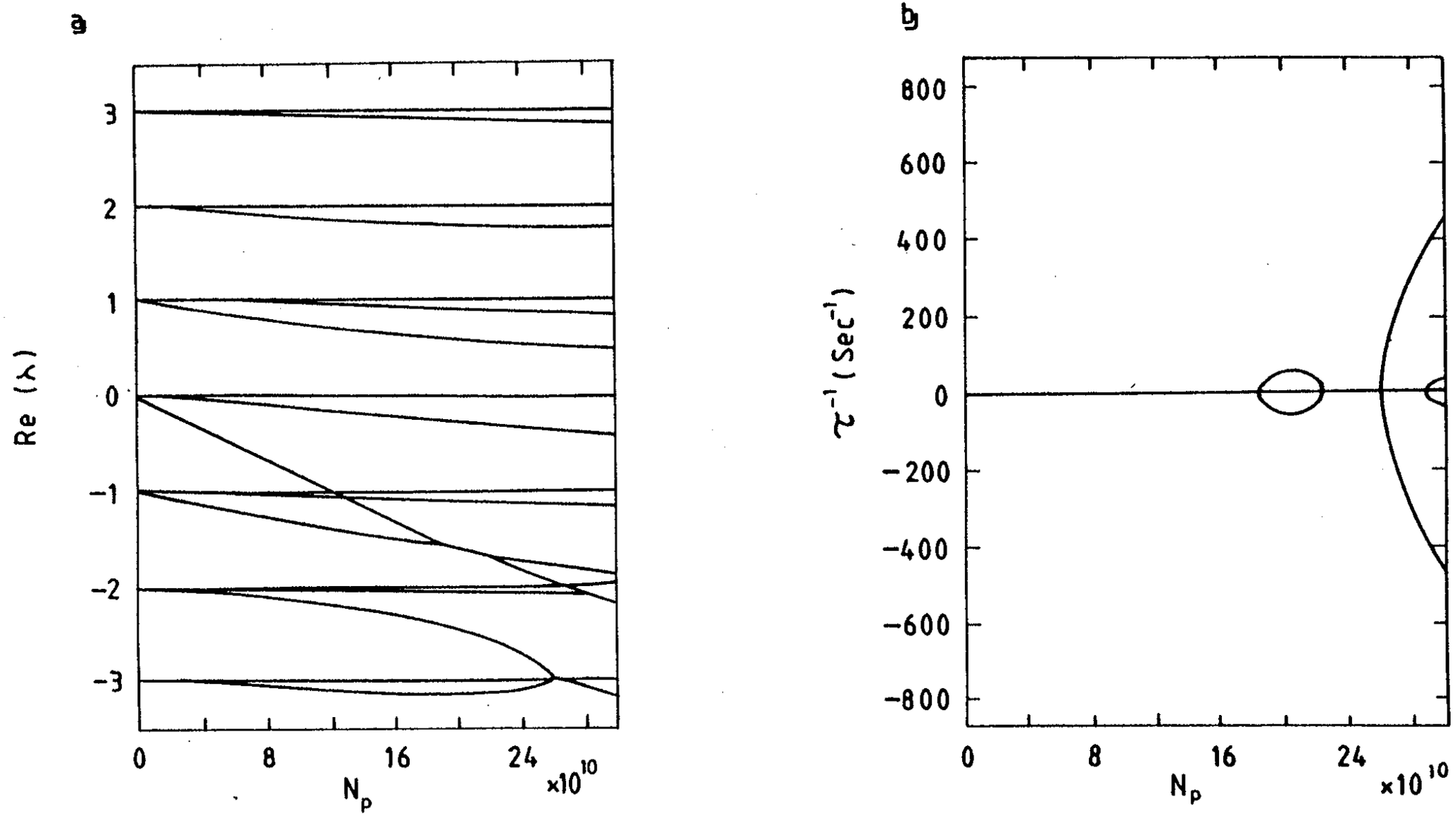

Fig. 6. Mode frequencies versus the number of particles in a bunch at 315 GeV(σ_z = 18 cm).
(a) Real part (b) Growth rate.

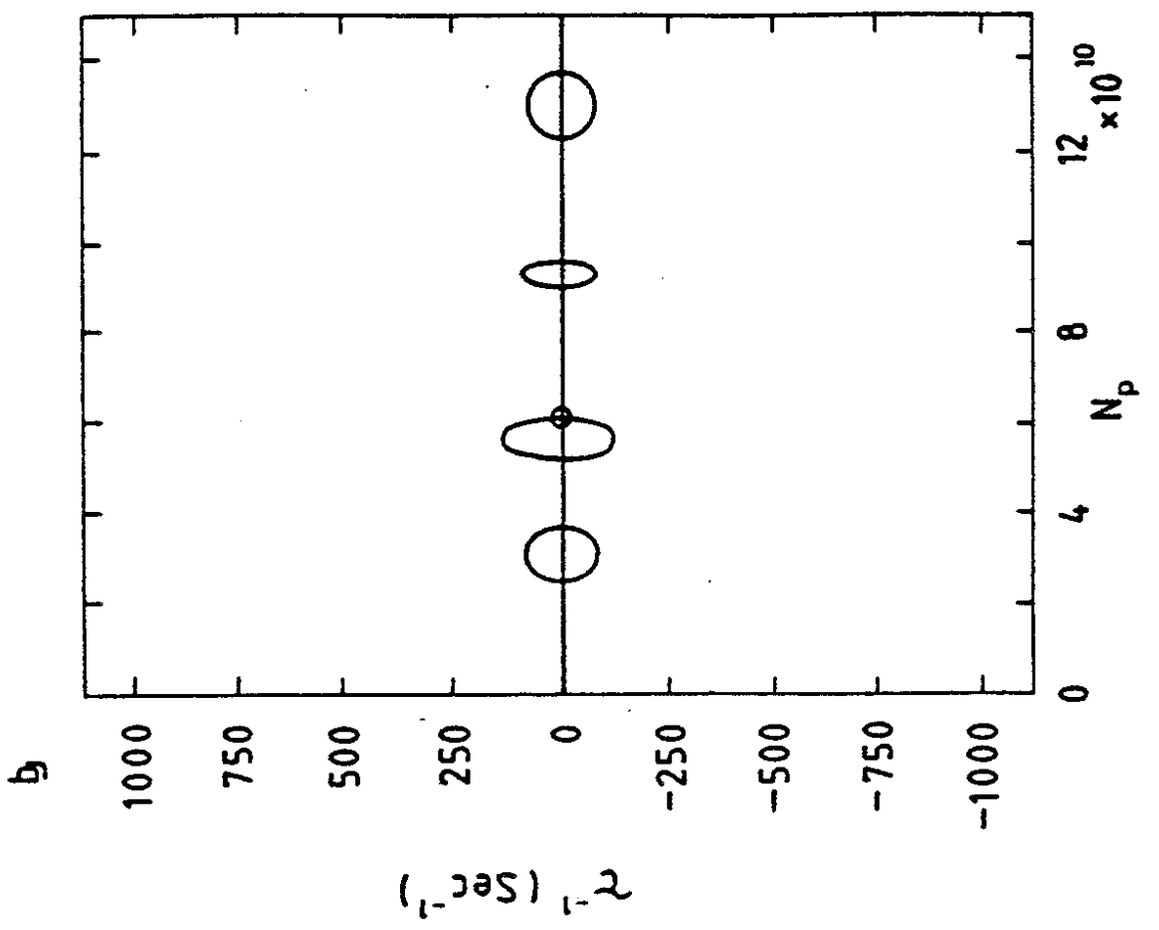

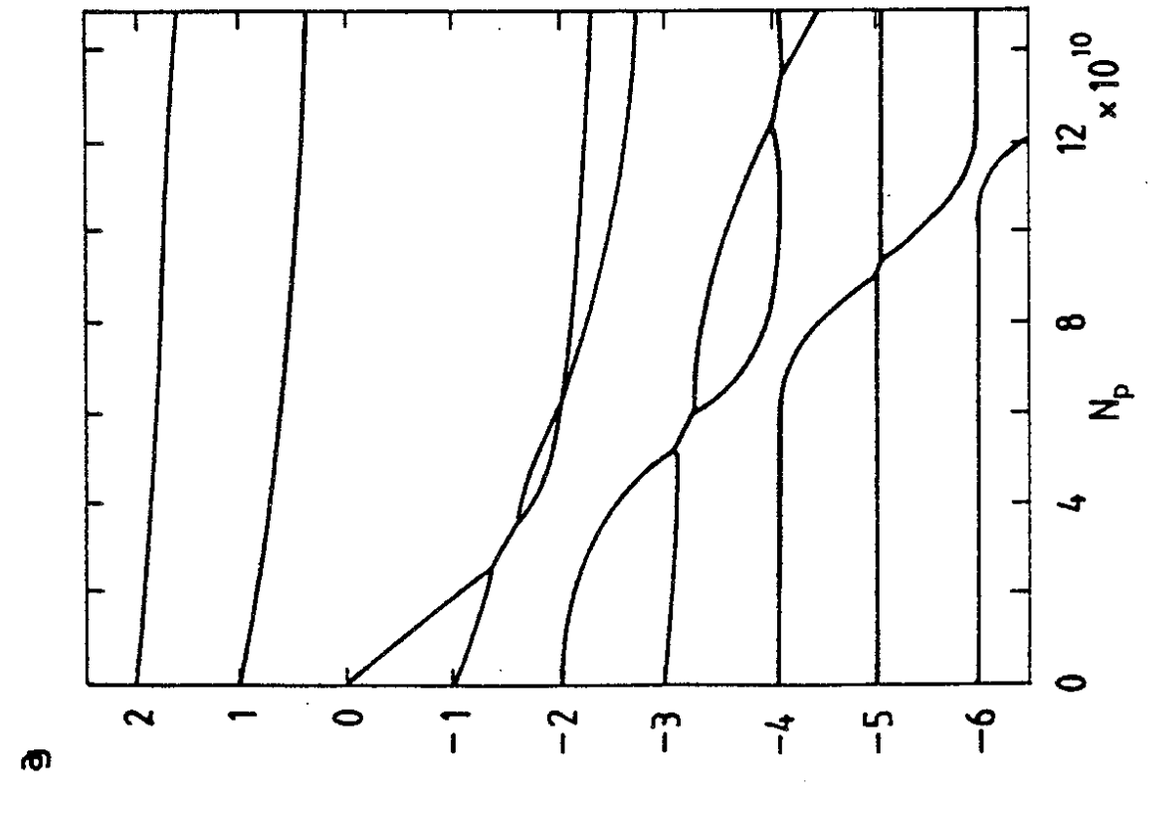

Fig. 7. Mode frequencies versus the number of particles in a bunch at 26 GeV (σ_z = 30 cm).
(a) Real part (b) Growth rate

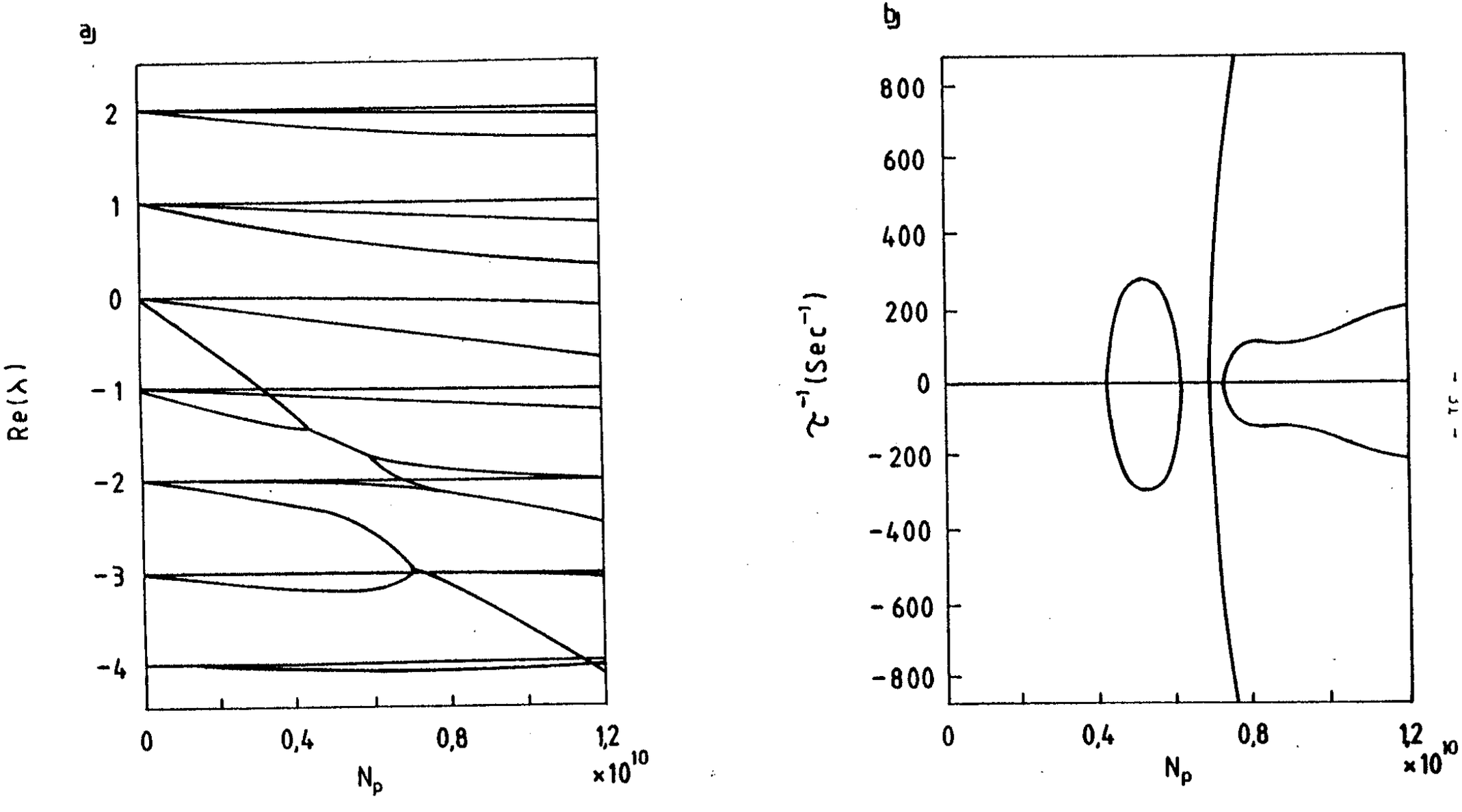

Fig. 8. Mode frequencies versus te number of particles in a bunch when operated as LEP injector at 3.5 GeV (σ_z = 16 cm)

(a) Real part (b) Growth rate

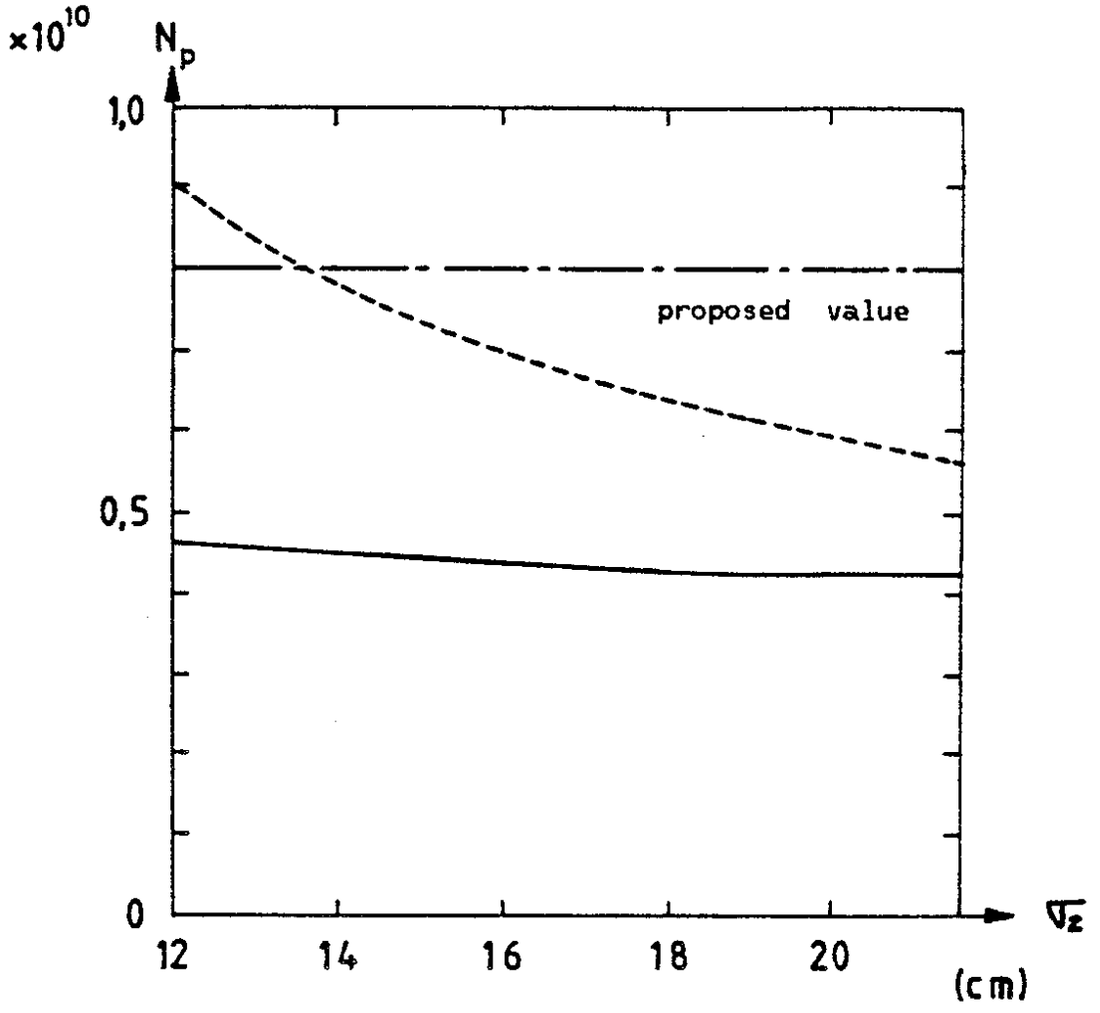

Fig. 9 Threshold beam intensity when operated as LEP injector for Z_T = 47.7 mΩ/m. The solid and the broken line show the thresholds due to coupling between m = 0 and m = -1 modes, and between m = -2 and m = -3 modes, respectively.